Journal of Anatomy ANATOMICAL SOCIETY WILEY

Intraspecific variation and directional casque asymmetry in adult southern cassowaries (*Casuarius casuarius*)

Todd L. Green[1,2] | David Ian Kay[2] | Paul M. Gignac[2,3,4,5]

[1]Department of Anatomy, New York Institute of Technology College of Osteopathic Medicine, Old Westbury, New York, USA

[2]Department of Anatomy and Cell Biology, Oklahoma State University Center for Health Sciences, Tulsa, Oklahoma, USA

[3]Department of Cellular and Molecular Medicine, University of Arizona College of Medicine, Tucson, Arizona, USA

[4]Division of Paleontology, American Museum of Natural History, New York, New York, USA

[5]MicroCT Imaging Consortium for Research and Outreach (MICRO), Fayetteville, Arkansas, USA

Correspondence
Todd L. Green, Department of Anatomy, New York Institute of Technology College of Osteopathic Medicine, Old Westbury, NY, USA.
Email: tgreen09@nyit.edu

Abstract

The cranial casques of modern cassowaries (*Casuarius*) have long intrigued researchers; however, in-depth studies regarding their morphological variation are scarce. Through visual inspection, it has been recognized that casque variability exists between conspecifics. Understanding casque variation has both evolutionary and ecological importance. Although hypothesized to be targeted by selection, intraspecific casque variation has not been quantified previously. Through a large sample of *C. casuarius* ($n = 103$), we compared casque shape (lateral and rostral views) between sexes and between individuals from non-overlapping geographical regions using two-dimensional (2D) geometric morphometrics. We found no statistically significant differences between the casque shape of females and males and few substantial shape differences between individuals from different geographic areas. Much of the intraspecific variation within *C. casuarius* is due to casque asymmetries (77.5% rightward deviating, 20.7% leftward deviating, and 1.8% non-deviating from the midline; $n = 111$), which explain the high variability of southern cassowary casque shape, particularly from the rostral aspect. Finally, we discuss how our non-significant findings implicate social selection theory, and we identify the benefits of quantifying such variation for further elucidating casque function(s) and the social biology of cassowaries.

KEYWORDS
cranial structure, geometric morphometrics, paleognathous birds, phenotypic variation, shape analysis, social selection, theropod, visual display

1 | INTRODUCTION

Birds are visually oriented organisms that use objects (e.g., bowers), colors, shapes, distributions of feathers, fleshy appendages, and hard-tissue ornaments for interspecific and intraspecific display (Gill, 2007). Body or cranial ornaments represent important ways that birds communicate their age,

sex, social status, reproductive capability, and species identity (Bolwig, 1973; Buchholz, 1991; Diamond, 1986; Frith, 1978; Gill, 2007; Hagelin, 2002; Jones & Hunter, 1999; Kemp, 2001; Kinnaird et al., 2003; Mayr, 2018; Raikow, 1969), and deciphering cranial structure meanings helps address how their functions impact avian behaviors, life histories, and evolution. For example, visually distinct integument and ornaments can assist

in distinguishing members of closely related species (Andersson, 1994). This appears to be the case for feather color patterns in birds like trogons (i.e., *Trogon*; Bitton & Doucet, 2016) and the headgear of artiodactyl mammals (Bubenik & Bubenik, 1990). The clear visual cues ornaments provide may also indicate whether a conspecific is a compatible mate by indicating that individual's sex (Darwin, 1871; Andersson, 1994) when closely related species share geographic distributions. Here, we focus on the cranial headgear of southern cassowaries (*Casuarius casuarius*), a flightless ratite and relative of ostriches, rheas, kiwis, and emus. Unlike their immediate living relatives, cassowaries are exceptionally conspicuous, possessing vividly colored apteria (e.g., blue, red, yellow, purple, white; Figure 1), carunculated skin, pendulous wattles, glossy feathers, and unmistakably prominent cranial casques. As a large and conspicuous structure, the casque in particular has long been a source of inquiry (e.g., Flower, 1871; Marshall, 1872; Parker, 1866; Pycraft, 1900; Rothschild, 1900). Nonetheless, few studies have formally addressed if and how this cranial adornment may serve as a visual display feature.

Compositionally, the casque of a southern cassowary contains an osteologically convoluted bony core (see Green & Gignac, 2021), as well as a thin, external sheathing of keratin. The bony core makes up the majority of casque volume, and the keratinous sheath influences the outer shape and color (e.g., black, gray, brown, green) of the structure. Cassowaries hatch without casques but proceed to expand and incorporate several cranial bones into the structure during ontogeny. Southern cassowaries have casques that consist of the mesethmoid bone and median casque element as well as the left and right nasals, lacrimals, and frontals (Green & Gignac, 2021). Primary casque growth in these birds begins at approximately 1.5 months of age and proceeds to the point at which sexual maturity is reached (Green & Gignac, 2021). Following this, casque enlargement appears to continue, albeit more slowly, throughout adulthood (Dodson, 1975; Green & Gignac, 2021). As a result of its bony complexity and relatively rapid growth (as compared to the rest of the head), there may be opportunities for variation in one or more of its bony components
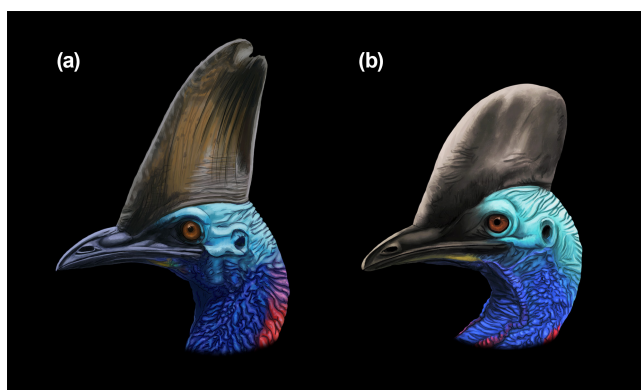
or outer keratin to contribute to overall variation in adult casque size or shape. In addition, casques are frequently asymmetrical in cassowaries (Perron, 2016; Rothschild, 1900). This can be particularly extreme in *C. casuarius* individuals (Rothschild, 1900), which tend to have casques that deviate laterally rightward or leftward of the midline (Figure 2).

Sexual dimorphism is common among birds, including cassowaries wherein females are approximately 30% larger than males (Olson & Turvey, 2013). In some avian species, sexual dimorphism has been detected specifically in cranial ornaments, such as the casques of guineafowl (*Numida*; Angst et al., 2020) and hornbills (e.g., *Bycanistes*, *Ceratogymna*; Kemp, 2001; Gamble, 2007), the fleshy knobs of curassows (i.e., *Crax*; Buchholz, 1991; Mayr, 2018), and the feather crests of peafowl (i.e., *Pavo*; Dakin, 2011). It has been hypothesized that the casques of *C. casuarius* may be sexually dimorphic (Crome & Moore, 1988; Hone et al., 2012; Naish & Perron, 2016; Rothschild, 1900), enabling females to be distinguished from males based on casque shape (e.g., relative tallness). If true, we hypothesize that sexes differ in casque shape, predictably. Support for this hypothesis would indicate that sexual dimorphism characterizes the *C. casuarius* casque, and sex may be an important source of variation for the casque phenotype.

Geographic segregation of conspecific populations can also result in opportunities for morphological divergences that increase variation. Morphological variation within a population may instigate subspecies divergences due to differential mating preference, survivorship, or fitness (Lande, 1976; Lande, 1979; Wright, 1945). In extreme cases, major population-level differences in phenotype or resultant behavior can lead to reproductively isolating members of the same species so much so that the populations can become reproductively incompatible (see Grant & Grant, 2009). Today, *C. casuarius* are widely distributed across several islands and mainland Australia. This is primarily the result of ancestral cassowary immigration across periodic land bridges between Australia, New Guinea, and smaller islands starting approximately 800,000 years ago (Naish & Perron, 2016). Glacially influenced sea level changes may have contributed to the geographic segregation of several populations of *C. casuarius* during this period (Naish & Perron, 2016). This history suggests that morphological variation in the casque may derive in part from the wide geographic distribution and regional isolation that *C. casuarius* experienced. If casque shape has evolved independently in these populations, then we hypothesize that shape differences within regional populations will be less than shape differences between regional populations, allowing for accurate categorization of *C. casuarius* subgroups based on casque shape. Support for this hypothesis would indicate that independent evolution due to geographic isolation may be an important source of *C. casuarius* casque variation.

Visually elaborate structures can function in multiple social contexts depending on behavior and audience, which could lead to differing display functions for the casque in different environments. Here, we formally examine adult casque shape variation across two scales of cassowary population organization in order to detect
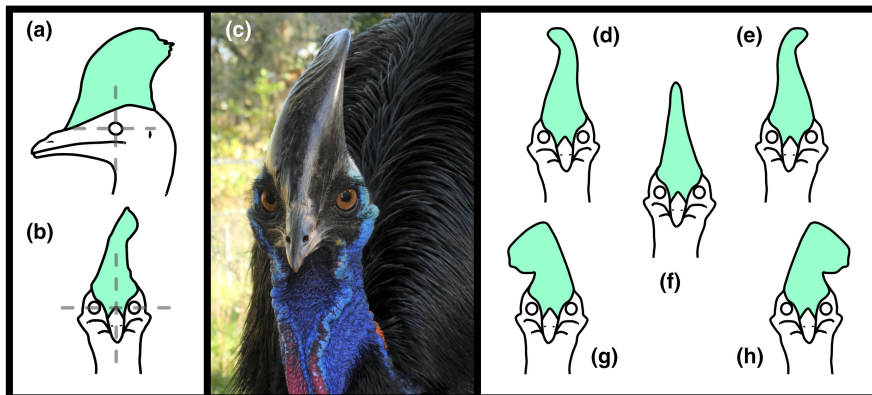

FIGURE 1 Illustrations depicting the phenotypic casque variation within *Casuarius casuarius* (a–b). Individuals are based on female representatives. Artwork by J. A. Campbell-Smith.

FIGURE 2 Cranial line illustrations of *Casuarius casuarius* (casques in pastel green) in lateral (a) and rostral views (b), the two anatomical aspects from which morphometric photographs were collected. Crosshairs were centered vertically and horizontally on the eye/orbit for lateral samples; alignment of the horizontal center of the eye/orbit and rostralmost boundary of the casque with the cranial midline was used for rostral samples (indicated by transparent gray dashed lines). Photograph illustrating casque asymmetry (c), a common anatomical feature in cassowaries. Casque asymmetries in *C. casuarius* manifest as either rightward sinusoidal (d), leftward sinusoidal (e), non-deviated (f), rightward (g), and leftward deviations (h) from the midline. Photo by T. L. G.
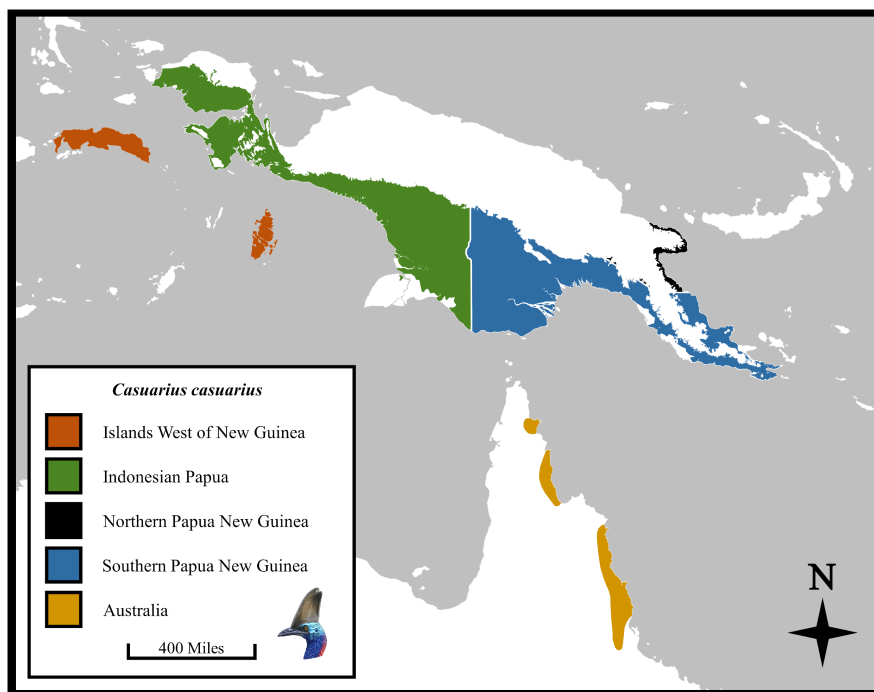

FIGURE 3 Map of Australasian *Casuarius casuarius* range with regional subdivisions based on historical and physical boundaries indicated on museum voucher tags (western islands near New Guinea = dark orange; Indonesian Papua = green; Northern Papua New Guinea = black; Southern Papua New Guinea = blue; Australia = dark yellow). Redrawn from BirdLife International (2019) geographical range data.

signals for display in life history and evolutionary contexts: (1) sexual dimorphism and (2) intraspecific geographic isolation. Our overall aim, therefore, is to determine if casque shape is consistent with between-sex and between-region hypotheses. We address each of these hypotheses by examining casque shape variation in a large, *C. casuarius* dataset. To accomplish this, we utilized photographic data collection, 2D geometric morphometrics, and elliptical Fourier analyses (EFAs; see Felice & O'Connor, 2014). Our findings do not support

sexual dimorphism nor structured geographic variation with the exception of an incipient pattern of independent casque evolution potentially due to geographic isolation of southern Papua New Guinea *C. casuarius* from those on the western islands near New Guinea. We conclude by discussing how our findings are consistent with social selection theory (West Eberhard, West-Eberhard, 1983; Schlupp, 2021) and its subset, mutual sexual selection theory (Hone et al., 2012; Huxley, 1914).

2 | METHODS

2.1 | Specimen sample

In total, 111 adult *C. casuarius* possessing intact keratinous sheaths were sampled for this study (see Supplemental Table). Photographs were taken of all individuals, including living animals, fluid preserved samples, dry skins, and skeletal preparations (with keratin preserved; see Supplemental Table). All 111 specimens were used to quantify casque asymmetry, and a subset of 103 individuals were sampled for 2D geometric morphometric shape analyses (see below). Specimens were obtained as vouchered from museum collections or as opportunistically collected cadaveric specimens after death. Specimen data were collected from the American Museum of Natural History (AMNH; New York, NY, USA), Brevard Zoo (BVZ; Melbourne, FL, USA), Cassowary Conservation Project (CCP; Fort Pierce, FL, USA), Denver Museum of Nature and Science (DMNS; Denver, CO, USA), Melbourne Museum (Museums Victoria, MV; Melbourne, VIC, AU), Museum of Osteology (MOO; Oklahoma City, OK, USA), Natural History Museum at Tring (NHMUK; Tring, UK), Queensland Museum (QM; Brisbane, QLD, AU), Sedgwick County Zoo (SCZ; Wichita, KS, USA), T. L. Green Research Collection (TLG; Tulsa, OK, USA), University of New England Natural History Museum, (UNE; Armidale, NSW, AU), and the Wet Tropics of Queensland (WTQLD; Cape Tribulation, QLD, AU, and Etty Bay, QLD, AU).

Adult status was ascertained via prior documentation of successful breeding activity, exclusively black plumage, and/or museum-voucher indication of maturity. Taxonomic determination of each *C. casuarius* specimen was based on a combination of previously established, species-specific anatomical characteristics, including wattle number, apteria coloration, and casque appearance (Marshall, 1872; Perron, 2016; Rothschild, 1900). Sex (*n* = 24 females, *n* = 35 males; see Supplemental Table) was determined based on museum voucher data, known breeding status, or sex-specific behavioral observations (e.g., males incubating eggs or rearing chicks, which are standard behaviors for male cassowaries; Crome, 1976).

We sampled wild-caught cassowary specimens for the geographic shape portion of this study and excluded individuals described as captive for all or part of their life (indicated by dashes in geography column of Supplemental Table). Specimens were collected broadly from across their known present-day and historical ranges (Rothschild, 1900; BirdLife International, 2019). However, geographic specimen data were not historically recorded for all specimens in our sample, and those that included collection regions often did not describe precise localities (see Supplemental Table). Nonetheless, the highest resolution spatial data possible were collected from each *C. casuarius* specimen. Each individual (*n* = 45) was categorized into a single broad geographic region: Australia (AUS), Indonesian Papua (INDP), southern Papua New Guinea (SPNG), and western islands near New Guinea (WIS) (Figure 3; see Supplemental Table). These regions represent populations that have experienced periodic geographic isolation from one another, including from the start of the Holocene to the present day (Naish & Perron, 2016 and references therein). We note that *C. casuarius* from islands west of New Guinea (i.e., Seram and Aru Islands) likely comprise native and introduced individuals (BirdLife International, 2019). Therefore, we combined the two islands into a single region for our analyses (Figure 3) because they potentially represent an admixture from other populations that cannot be accounted for. We also discounted specimens with locality data that were geographically too broad (e.g., "New Guinea"). Finally, *C. casuarius* is found in a relatively small region of northern Papua New Guinea (Figure 3); however, we did not sample any individuals known to have come from this region. Modern range distribution data for *C. casuarius* were used with permission from BirdLife International (2019).

2.2 | Photographic data collection

No institutional animal care and use protocol was required for this study. Only non-intrusive, photographic data were obtained with organization permission from captive specimens (BVZ, CCP) and wild birds (WTQLD), which required no direct interaction with the animals. Photographs for morphometric analyses (see next) were collected by T. L. G. using a Panasonic DMC-ZS60, Leica DC Vario-Elmar 1:3.3–6.4/4.3–129 ASPH Lens (Panasonic Corporation, Kadoma, JP; Leica Microsystems, Wetzlar, GER) and a Canon EOS D60, Tamron SP 200–500 mm F/5.0–6.3 Lens (Canon Inc., Tokyo, JP; Tamron Corp., Saitama, JP). Photographs were taken at ≥1.0 m distance from each sample with solid-contrasting backgrounds (when possible) to ensure visibility of casque outlines. Of the 111 vouchered and living specimens that were photographed, 107 were photographed with the Panasonic DMC-ZS60 and Leica DC Vario-Elmar 1:3.3–6.4/4.3–129 ASPH Lens except for those taken of living cassowaries at WTQLD (*n* = 4), which were collected using the Canon EOS D60 and Tamron SP 200-500 mm F/5.0–6.3 Lens. Photos of living cassowaries were collected behind chain-link fencing at BVZ and CCP and with a telephoto lens (but no barrier) at WTQLD, both of which served to ensure safely for the observer. To avoid potential image distortion due to the use of two lenses, we standardized the photography protocol following steps for common specimen framing, alignment, and position recommended by Marugán-Lobón and Buscaliono (Marugán-Lobón & Buscalioni, 2004). Specimens were photographed individually with each head centered, occupying <50% of the frame, and with all anatomical structures of interest in focus and absent from the image edges. Specifically for lateral photographs, crosshairs were centered upon the middle of the orbit (e.g., using the center of the eye in lateral gaze as a reference when present). For rostral photographs, crosshairs were centered upon on the rostralmost midpoint of the casque, aligned with the midpoint of the orbit (Figure 2a,b). Depending on the condition of the casques and access to all casque orientations for collecting photographs and measurements, some known-sex specimens were not used in all analyses (see sex breakdown for each respective section).

2.3 | 2D geometric morphometric analyses

Only those sampled cassowaries with undamaged and non-pathological casques (e.g., without sections of casque broken off in life) were included in the 2D geometric morphometric analyses, 103 in all. One hundred and one lateral- and 87 rostral-view photographs were used to assess 2D shape differences across these 103 individuals (no more than one photograph each in lateral and rostral view per individual was used; see Supplemental Table). In some instances, casques were suitable for one view (lateral or rostral) and not the other due to slight damage (i.e., keratin flaking) or physical access to all sides of a specimen. Photos were imported into Microsoft PowerPoint 365 (Microsoft Corp., Redmond, WA, USA) and closed outlines were traced using the Bézier curve tool. The resulting shapes were filled (which created a standardized, straight-lined casque base from rostralmost to caudalmost edges in lateral view, or from right to left lateral edges in anterior view, to standardize the ventral casque margin), saved as Portable Network Graphics files (PNGs), converted to a binary mask in ImageJ (v. 1; US National Institutes of Health, Bethesda, MD), and exported as Joint Photographic Experts Group files (JPGs). Most ($n = 90$) of the lateral shapes were drawn from photos taken of the left side of the animal; however, 11 individuals were photographed from the right side only. The right-lateral casque shapes were mirrored before combining with those from the left side. In order to confirm that left- and right-mirrored casques could be accurately pooled together for analysis, we compared a random subset of shapes from 20 *C. casuarius* that were photographed from both left and right sides. We removed the effects of orientation, location, and scale from the outline data via landmark assignment of the most rostroventral and posteroventral points of the casque outlines, which were registered as Bookstein coordinates to establish them as a baseline (using the coo_bookstein function in *Momocs*). We then quantified outline shape using an EFA, ordinated the resultant harmonic data (see Supplemental Figure) using a principal coordinate analysis (PCOa), conducted a multivariate analysis of variance (MANOVA) with the principal coordinate scores to test for significant differences between left- and right-mirrored casque shapes, and evaluated the classifiability of left- and right-mirrored shape data with a linear discriminant analysis (LDA) on the principal coordinate scores (for specifics, see more detailed workflow below; see Supplemental Material for R code). The PCOa for *C. casuarius* left- and right-mirrored lateral casque shapes resulted in 38 principal coordinates with the first two capturing 87.3% of the total shape variation (PCO1 = 62.8%; PCO2 = 24.5%). Eight axes were retained for the MANOVA as they explained 99.0% of data variance. The MANOVA failed to detect a significant difference ($\alpha = 0.01$) between left- and right-mirrored casques ($p = 0.957$). Linear discriminant analysis results for lateral casque shapes indicate an overall cross-validation rate of 57.5% with 60.0% accuracy for left casque shapes and 55.0% accuracy for right-mirrored casque shapes. The LDA on the PCOa results indicates that shape predicts left- versus right-mirrored shapes about as well as random

chance. These results provide a justification for combining the 11 mirrored right lateral shapes with the left lateral shapes in our formal analyses.

We also tested for outliers in the entire casque shape outline set, using the *Momocs* package (Bonhomme et al., 2014) in R (v 3.6.3; R Core Team, 2020) to identify outliers in the lateral and rostral outline data (Supplemental Material for R code). Two potential shape outliers were flagged from the rostral outlines (neither of these flagged individuals were right-mirrored lateral-casque tracings). These individuals (MOO 8031, NHMUK 1916.5.30.1483) were re-evaluated for labeling issues, tracing errors, photographic artifacts, and pathologies. None were identified; therefore, it was determined that these specimens were likely flagged because they have rarer shapes for *C. casuarius* compared to overall shape space (e.g., particularly deviated from midline). Therefore, we recognize these individuals as statistical—not biological—outliers and did not remove them from the analyses. Below we account for incorporation of statistical outliers in our MANOVAs.

It is also possible that casque shape differences between sexes from more localized populations may have been masked by including all regions in one analysis. To address this, we also tested for sexual dimorphism at geographic localities for which there were enough known-sex individuals with undamaged and non-pathological casques to perform statistical tests (i.e., AUS, SPNG). This was done by taking the quantified shape data (see above), ordinating it with principal component analysis (PCA), and running MANOVAs to test for significant differences between sexes at each location in lateral (AUS, $n = 6$ females, $n = 8$ males; SPNG, $n = 3$ females, $n = 4$ males) and rostral views (AUS, $n = 4$ females, $n = 5$ males; SPNG, $n = 3$ females, $n = 4$ males). None of these comparisons yielded significant results ($\alpha = 0.01$; $p > \alpha$). This indicates that combining individuals of different locations in our dataset does not bias shape variation in favor of females or males nor introduce novel ranges of variation that could skew results of the entire sample.

Following our data inspection procedures, we ran four primary shape analyses in total. In our lateral-view casque shape analyses, we tested two factors: (1) sex ($n = 23$ females, $n = 30$ males) and (2) geographic region in ($n = 20$ AUS, $n = 8$ INDP, $n = 9$ SPNG, $n = 8$ WIS). In our rostral-view casque shape analyses, we tested the same two factors: (1) sex ($n = 18$ females, $n = 24$ males) and (2) geographic region ($n = 15$ AUS, $n = 6$ INDP, $n = 9$ SPNG, $n = 7$ WIS). All shape quantification and statistical analyses were completed in R (v 3.6.3; R Core Team, 2020) using the *Vegan*, *MASS*, and *Momocs* packages (Bonhomme et al., 2014; Oksanen et al., 2007; Ripley, 2013). For our four primary shape analyses, we employed several of the same steps described previously in the mirrored-casques comparison. We imported, assigned, and converted casque shapes into coordinate outlines, followed by aligning (i.e., orienting, scaling, and centering) our binary casque shape outlines via landmark assignment. Alignments registered the rostroventral and posteroventral edges of the casque outlines as Bookstein coordinates to establish them as a baseline (using the coo_bookstein

function in *Momocs*). Once aligned, casque outlines were quantified using EFAs. Elliptical Fourier analyses were selected for this study because the casques of adult cassowaries do not have easily placed homologous landmarks, particularly on the distal areas of interest. Instead, EFA uses x-y coordinates as semi-landmarks and quantifies shape with harmonic variables. The number of harmonics was chosen to capture 99.9% of casque shape (i.e., 14–16 harmonics for each analysis; 16 for lateral sex, 14 for rostral sex; 15 for lateral geographic region, and 14 for rostral geographic region) while maintaining statistical power by assigning fewer harmonics than samples tested. Harmonic data were ordinated by conducting PCAs. The principal component (PC) scores were plotted to visualize and inspect the resultant morphospace and convex hulls of grouping factors for each analysis (i.e., sex or geographical region). Using PC-score data representing 99.0% of variance (6–9 axes), MANOVAs were run to test for significant differences ($\alpha = 0.01$) between casques. Pairwise MANOVAs were used to test the comparisons between grouping factors. Alpha values of 0.01 were chosen for all MANOVAs to reduce the potential for Type I error, which could be inflated by including statistical outliers and inconsistent sample sizes in our analyses. These alpha values were also selected to account for compounding error from multiple comparisons. Linear discriminate analyses were run to evaluate the ability of the different groups within each factor to be classified given their shape data.

In order to better interpret our *C. casuarius* rostral shape output results for sex and geography, we additionally analyzed and categorized casque asymmetry. *Casuarius casuarius* casques grow from unpaired bones located along the midline (mesethmoid and median casque element) as well as paired bones located immediately parasagittal to the midline (frontals, lacrimals, and nasals), superimposed by tightly adhering keratin (Green & Gignac, 2021). Casque initiation and early inflation tends to align with the midsagittal axis. However, adult casques commonly deviate from the midline (Rothschild, 1900; Perron, 2016; Figure 2c–h), taking on left- or right-sided convexities as they mature with the dorsalmost aspect of the casque sometimes deviating dramatically to either side.

To capture casque variations as they relate to deviation, we assessed asymmetries in all wild and captive *C. casuarius* specimens from rostral-view photographs (Figure 2b). First, we documented broad asymmetries categorically (non-deviated, leftward, rightward, sinusoidal leftward, sinusoidal rightward) from all 111 individuals. Sinusoidal casques are those that deviate in one direction at the anteroproximal base only to recurve on themselves to deviate in the other direction at the distal tip. Next, using degree asymmetries, we compared deviation from vertical (=0° at the midline of the rostrum) in transverse orientation (rostral-view images) for 88 specimens (Figures 2d–h, 4). (Note, this is one more individual than was sampled for the rostral-view 2D geometric morphometric analysis. That individual, QM O.3435, possessed casque keratin with excessive postmortem peeling that precluded shape tracing but did not preclude measuring
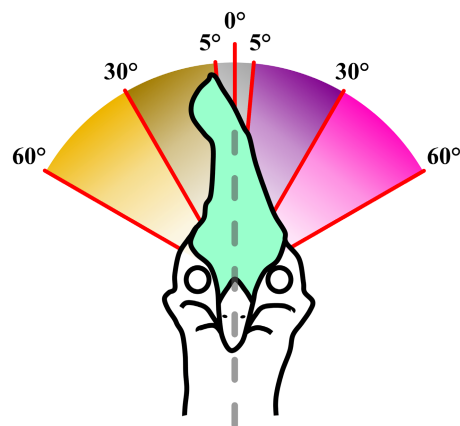

FIGURE 4 Methods for determining degrees of deviation categories (none–minimal, 0°–5° leftward/rightward = gray; slight–moderate rightward, 6°–30° = dark gold); slight–moderate leftward, 6°–30° = dark purple; severe–radical rightward, 31°–60° = light gold), and (5) severe–radical leftward, 31°–60°; = light purple) for *Casuarius casuarius* casques in rostral view (pastel green).

asymmetry.) The measurement for casque deviation angle (to the nearest 1°) was taken between two lines that connect three points: (1) from the midsagittal plane from above the orbits, (2) to the rostralmost casque base, (3) to the lateralmost point of the deviated dorsal casque surface. (Note, this measurement ignores the previously mentioned sinuous topology.) Categorical and by-degree asymmetries from 43 known-sex individuals were also compared (n = 19 females, n = 24 males) to evaluate sexual dimorphism in casque deviation. Examining casque deviations using two metrics enabled us to capture overall deviations as well as within-deviation morphologies that seem common among cassowaries.

3 | RESULTS

3.1 | Casque shape—sex

The PCA for known-sex lateral casque shapes resulted in 53 principal components with the first two capturing 85.5% of the total shape variation (PC1 = 61.2%; PC2 = 24.3%; Figure 5). The PCA for known-sex, rostral casque shapes resulted in 42 principal components with the first two capturing 83.1% of the total shape variation (PC1 = 53.6%; PC2 = 29.5%; Figure 6). Convex hulls around female and male PC scores overlap substantially in morphospace plots for both lateral and rostral PCAs, respectively (Figures 5, 6), suggesting the female and male casques share similar shapes and shape variances. Multivariate analysis of variances for known-sex, lateral and rostral casques yielded non-significant results ($p > \alpha$; Table 1), indicating that neither lateral nor rostral casque shape differences are apparent between adult *C. casuarius* females and males. Linear discriminant analysis results for known-sex, lateral casques indicate an overall cross-validation rate of 60.4% with 60.9% accuracy for
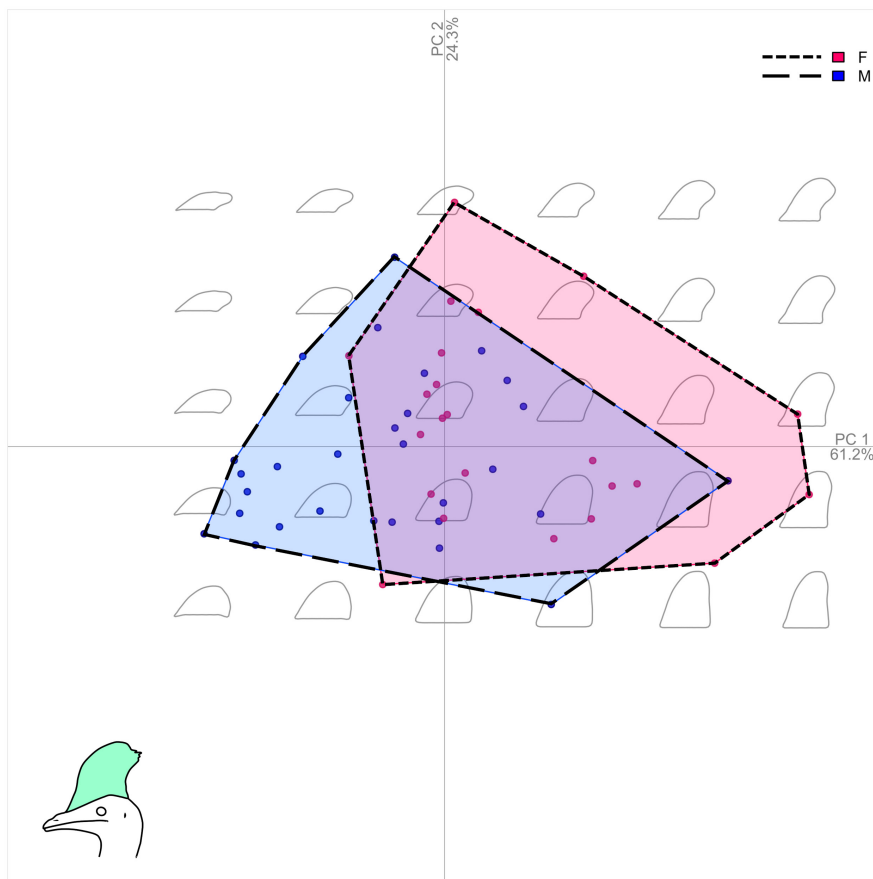
FIGURE 5 Output of the PCA comparing lateral casque outlines between sexes (female = pink datapoints and polygon; male = blue datapoints and polygon) of *Casuarius casuarius* (pastel green casque icon at lower left). Female and male convex hulls illustrate substantial overlap in lateral casque morphospace between the sexes. Theoretical casque shape based on the principal component axes shown as gray outlines.

females and 60.0% accuracy for males (Table 2). Linear discriminant analysis results for rostral casque shapes indicate an overall cross-validation rate of 57.1% with 33.3% accuracy for females and 75.0% accuracy for males (Table 2). The results of the MANOVAs are not significantly different, and the LDA results indicate that shape predicts sex about as well as random chance. These findings fail to support our hypothesis that sex can be predicted from casque shape in *C. casuarius*.

3.2 | Casque shape—geography

The PCA for known-geography, lateral casque shapes resulted in 45 principal components with the first two capturing 88.5% of the total shape variation (PC1 = 66.6%; PC2 = 21.9%; Figure 7). The PCA for known-geography, rostral casque shapes resulted in 37 principal components with the first two capturing 84.1% of the total shape variation (PC1 = 50.2%; PC2 = 33.9%; Figure 8). Convex hulls around AUS, INDP, SPNG, and WIS PC scores overlap substantially in morphospace plots for both lateral and rostral PCAs, respectively (Figures 7, 8), suggesting regional groups share similar shapes and shape variances. Multivariate analysis of variances and pairwise

comparisons for *C. casuarius* known-geography, lateral and rostral casque shapes generally yielded non-significant results ($p > \alpha$ values; Table 1). The exception was a significant p-value in a pairwise comparison between rostral SPNG and WIS. This result indicates that SPNG and WIS cassowaries in our sample differ in just a single view (rostral), whereas the rest of the sampled *C. casuarius* populations share similar overall shapes. Linear discriminant analysis results for known-geography, lateral casque shapes indicate an overall cross-validation rate of 64.4% with 80.0% accuracy for AUS, 37.5% for INDP, 44.4% for SPNG, and 75.0% for WIS (Table 2). Linear discriminant analysis results for rostral casque shapes indicate an overall cross-validation rate of 48.6% with 60.0% accuracy for AUS, 33.3% for INDP, 44.4% for SPNG, and 42.9% for WIS (Table 2). The LDA results indicate that shape consistently predicts geography poorly. The finding fails to support our hypothesis that geographic locality can be reliably predicted from casque shape in *C. casuarius*.

3.3 | Casque asymmetry

Casques were non-deviated in 1.8% of the total sample ($n = 111$), deviated to the left (leftward and leftward sinusoidal) in 20.7%
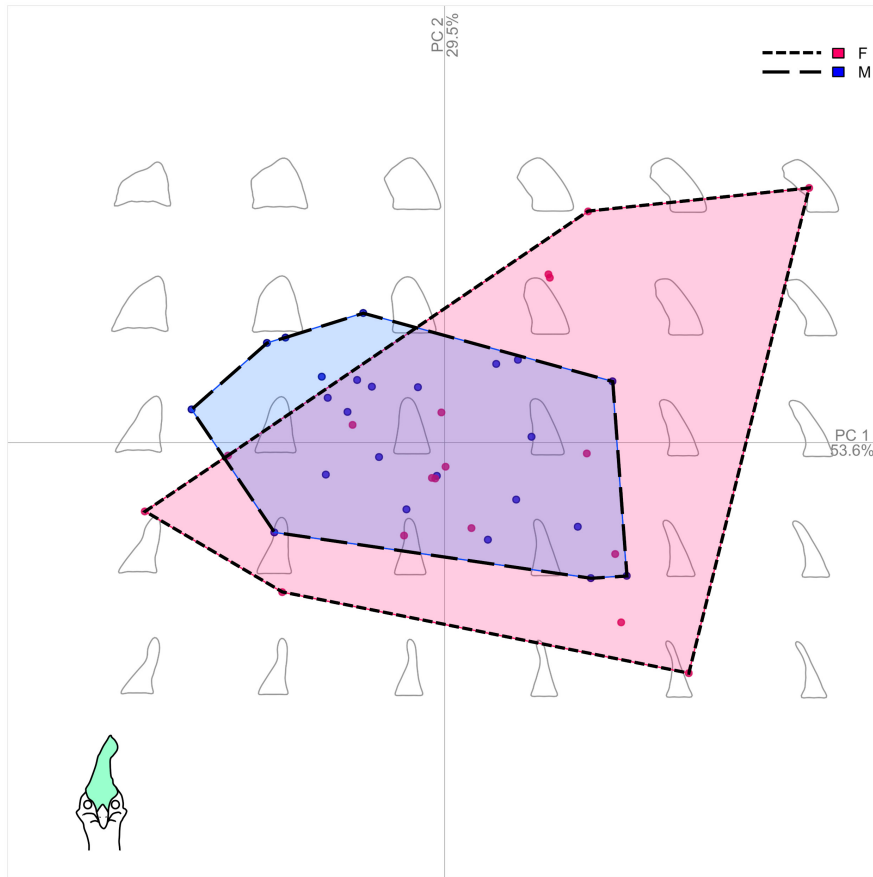
FIGURE 6 Output of the PCA comparing rostral casque outlines between sexes (female = pink datapoints and polygon; male = blue datapoints and polygon) of *Casuarius casuarius* (pastel green casque icon at lower left). Female and male convex hulls illustrate substantial overlap in rostral casque morphospace between the sexes. Theoretical casque shape based on the principal component axes shown as gray outlines.

of the sample, and deviated to the right (rightward and rightward sinusoidal) in 77.5% of the sample (see Supplemental Table). For ease of discussion, quantitative degree measurements are referred to here as either (1) none–minimal leftward or rightward (0–5° left or right), (2) slight–moderate leftward (6–30° left), (3) slight–moderate rightward (6–30° right), (4) severe–radical leftward (31–60° left), and (5) severe–radical rightward (31–60° right) (Figure 4; see Supplemental Table). Quantitatively, casques of 60.2% of our *C. casuarius* sample (*n* = 88) had slight–moderate rightward deviations from midline, whereas 22.7% showed none–minimal deviations, 9.1% showed severe–radical rightward deviations, 6.8% showed slight–moderate leftward deviations, and only 1.1% showed severe–radical leftward deviations (Figure 9). A comparable number of individuals from each sex (*n* = 19 females, *n* = 24 males) had slight–moderate deviations (68.4% and 75.0%, respectively) regardless of side. Among severe–radical deviations, females were substantially over-represented as compared to males (26.3% and 4.2%, respectively), whereas among none–minimal deviations, males were more commonly represented than females (20.8% and 5.3%, respectively; Figure 10). Although we documented several examples of sinusoidal casques, there were no phenotypes in the sample for which casque morphology was

both sinusoidal and the overall angular measurement of the asymmetry was non-deviated.

4 | DISCUSSION

We examined casque variation in *C. casuarius* from three perspectives: between female and male casque shapes, between geographic region casque shapes, and among casque asymmetries. Our findings generally showed non-significant differences in casque shapes, but with one exception. Here, we consider what these findings mean for interpretations of cassowary biology and geographic history.

4.1 | Sex-specific casque shape variation

Adult female and male cassowaries are body size dimorphic. Fully grown *C. casuarius* females are approximately 30% larger in body mass than their fully grown male counterparts (see Olson & Turvey, 2013). This has likely led to speculation as to whether *C. casuarius* casques are also dimorphic (Crome & Moore, 1988; Hone et al., 2012; Naish & Perron, 2016; Rothschild, 1900). Despite

TABLE 1 MANOVA outputs for *Casuarius* shape data

MANOVA	Pairwise test	Degrees of freedom	F-value	p-value
Sex (*C. casuarius*) – Lateral	—	52	2.287	0.034
Sex (*C. casuarius*) – Rostral	—	41	1.369	0.243
Geography (*C. casuarius*) – Lateral				
	AUS–INDP	27	1.946	0.111
	AUS–SPNG	28	1.596	0.188
	AUS–WIS	27	3.608	0.010
	INDP–SPNG	16	1.480	0.296
	INDP–WIS	15	6.530	0.011
	SPNG–WIS	16	2.544	0.104
Geography (*C. casuarius*) – Rostral				
	AUS–INDP	20	3.049	0.040
	AUS–SPNG	23	4.062	0.010
	AUS–WIS	21	2.108	0.113
	INDP–SPNG	14	4.104	0.035
	INDP–WIS	12	2.835	0.115
	SPNG–WIS	15	6.965	0.005*

Note: Degrees of freedom denotes the sum of factor and residual degrees of freedom. * = significant difference ($\alpha = 0.01$). All values are rounded to the nearest thousandth. Those values that read 0.010 are greater than the alpha value but are rounded down in table due to significant figures.
Abbreviations: AUS, Australia; INDP, Indonesian Papua; SPNG, southern Papua New Guinea; WIS, islands west of New Guinea.

TABLE 2 LDA results for *Casuarius* shape data

LDA					
Sex (*C. casuarius*)		Predicted as			
			Female	Male	
	Known identity	Female	LAT = 0.609	LAT = 0.391	
			ROS = 0.333	ROS = 0.667	
		Male	LAT = 0.400	LAT = 0.600	
			ROS = 0.250	ROS = 0.750	
Geography (*C. casuarius*)		Predicted as			
			AUS	INDP	SPNG	WIS
	Known identity	AUS	LAT = 0.800	LAT = 0.050	LAT = 0.050	LAT = 0.100
			ROS = 0.600	ROS = 0.200	ROS = 0.000	ROS = 0.200
		INDP	LAT = 0.375	LAT = 0.375	LAT = 0.125	LAT = 0.125
			ROS = 0.333	ROS = 0.333	ROS = 0.167	ROS = 0.167
		SPNG	LAT = 0.333	LAT = 0.111	LAT = 0.444	LAT = 0.111
			ROS = 0.333	ROS = 0.111	ROS = 0.444	ROS = 0.111
		WIS	LAT = 0.000	LAT = 0.125	LAT = 0.125	LAT = 0.750
			ROS = 0.571	ROS = 0.000	ROS = 0.000	ROS = 0.429

Note: Results of linear discriminant analyses (LDAs) comparing principal components of *Casuarius casuarius* casque outlines (lateral = LAT; rostral = ROS) between sexes (female and male) and between geographical regions (Australia = AUS, Indonesian Papua = INDP, Southern Papua New Guinea = SPNG, and Western Islands near New Guinea = WIS). The LDA was unable to consistently classify casque shape between sexes and was unable to consistently classify casque shape between geographical regions. Values are rounded to the nearest thousandth.

substantial variability between the casques of *C. casuarius* individuals generally, we did not find significant differences in lateral or rostral casque shapes ($p = 0.034$ and 0.243, respectively) between females and males (Tables 1, 2; Figures 5, 6). Indeed, female and male cassowaries appear to possess relatively similar external features, such as skin color, wattles, and feather patterns. Consistent with
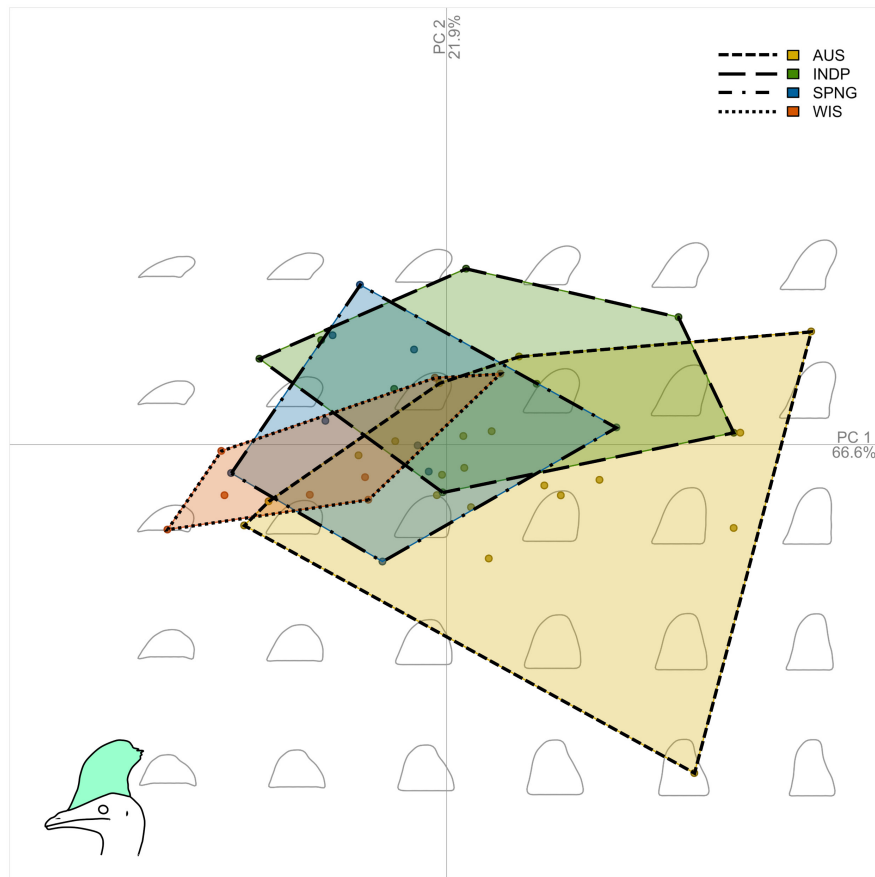
FIGURE 7 Output of the PCA comparing lateral *Casuarius casuarius* (pastel green casque icon at lower left) casque outlines between geographical regions: Australia (AUS = dark yellow), Indonesian Papua (INDP = green), Southern Papua New Guinea (SPNG = blue), and Western Islands near New Guinea (WIS = dark orange). Geographic convex hulls illustrate substantial overlap in lateral casque morphospace between the regions. Theoretical casque shape based on the principal component axes shown as gray outlines.

these morphometric traits, our study indicates that casque shape is also not readily distinguishable between sexes. For example, adult females of moderate sizes, which are comparable to those of adult male cassowaries, do not appear to have casques with female-specific shapes. Specifically, our cross-validation analyses accurately classify 75.0% of male casques based on rostral shape data (likely due to less deviated casques). However, our results simultaneously preclude the opportunity for distinguishing sex based on casque shape in those females that have not achieved maximum size, which is supported by the substantially lower, 33.0%, accurate classification for females. Adult females of large sizes, on the other hand, also have large casques. The casque may contribute to this apparent overall size advantage enjoyed by massive females by enabling these large birds to appear even larger.

The lack of casque shape dimorphism suggests that, if the casque is used for visual signaling, the signal may therefore not be sex specific. For example, intraspecific size differences are important to cassowary social interactions, especially regarding territorial aggression and courting behaviors (Bentrupperbaumer, 1997). In these cases, cassowaries (female and male) tend to compare body sizes, visually, using a stretch display. By standing as

tall as possible, total height is evaluated as a proxy for quality (Crome, 1976; also see Bolwig, 1973) with taller individuals maintaining dominance (Bentrupperbaumer, 1997). Consistent with our findings that females and males possess comparably shaped casques, we propose an alternative visual display function for the casque as a feature to enhance apparent tallness and, thus, help to establish the dominance of taller individuals. Notably, southern cassowary casques achieve most of their dorsoventral expansion by the time a bird reaches sexual maturity (Green & Gignac, 2021), which is also when dominance behaviors over territory and mates become the most selectively advantageous (Bentrupperbaumer, 1997).

4.2 | Geography-specific casque shape variation

We also tested for shape differences between geographically segregated populations. Geographic isolation may contribute to casque shape variation by enabling within-population shape changes that are not reflected in non-continuous or non-interbreeding groups. Notably, subspecies interpretations among *C. casuarius* involve
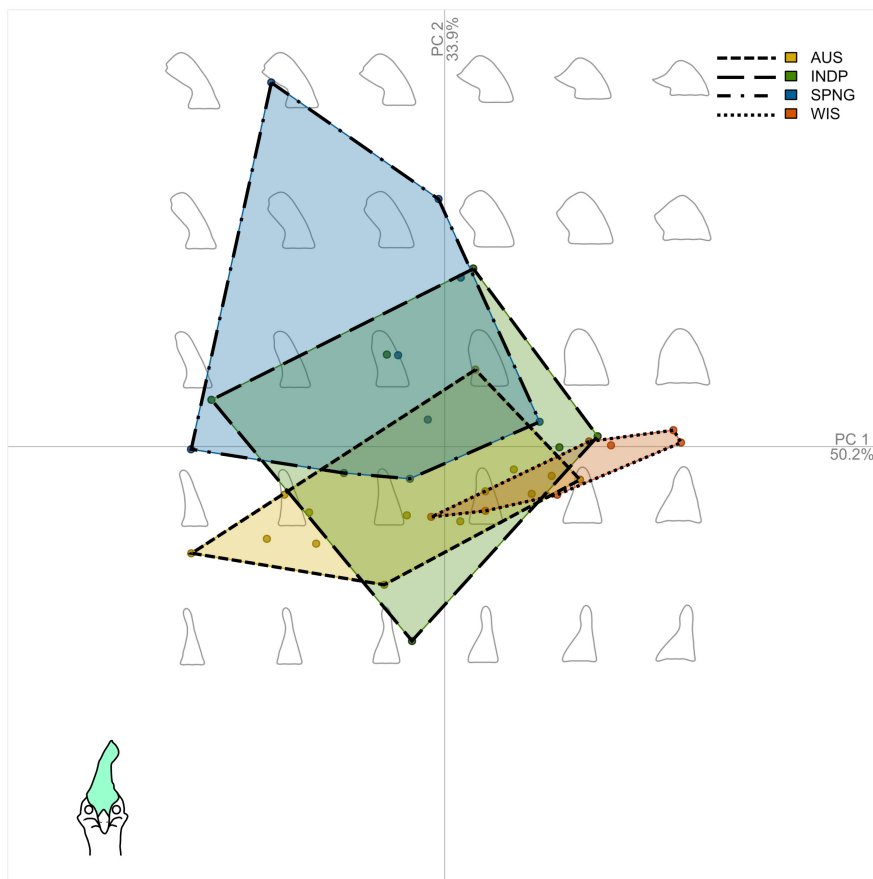
FIGURE 8 Output of the PCA comparing rostral *Casuarius casuarius* (pastel green casque icon at upper left) casque outlines between geographical regions: Australia (AUS = dark yellow), Indonesian Papua (INDP = green), Southern Papua New Guinea (SPNG = blue), and Western Islands near New Guinea (WIS = dark orange). Geographic convex hulls illustrate substantial overlap in rostral casque morphospace between the regions. Theoretical casque shape based on the principal component axes shown as gray outlines.

distinguishing traits like region-specific apteria coloration, whereas the inclusion of casque morphologies has been contentious (Naish & Perron, 2016; Perron, 2016; Rothschild, 1900). Our lateral-view sample demonstrated no signal of regionalized shape disparity. Instead, we found that regional groups share similar shapes and shape variances (Table 1; Figures 7, 8), with one exception.

Rostral casque shapes differed significantly between the southern Papua New Guinea and western islands near New Guinea regional populations ($p = 0.005$; Tables 1, 2; Figure 8). No other rostral-view, regional-population pairings were significantly different. These findings suggest that casque variation can harbor a regional signature, albeit a relatively weak one in our overall sample. Our data are, at best, ambiguous as to whether casque shape could be reliable for some subspecies designations. We would also caution that the complexities of biogeographical changes in sea level as well as centuries of human trade may have obscured genetic and morphological variation across *C. casuarius* (Perron, 2016). For example, *C. casuarius* on Seram (Perron, 2016; BirdLife International, 2019; IUCN, 2020) are thought to have dispersed partially or fully through human introduction. We cannot, therefore, discount that our findings may reflect an effect of human-governed dispersal patterns on cassowary phenotypic disparity. Genetic comparisons alongside

additional morphological and behavioral studies with larger sample sizes are needed to formally evaluate if these casque features distribute predictably among more closely related *C. casuarius* populations.

4.3 | Casque asymmetries

Cranial asymmetries are relatively common in some vertebrate skulls, such as those of crossbills (i.e., *Loxia*, Benkman, 1996), 'akepa (*Loxops*; Hatch, 1985), owls (e.g., *Aegolius*, *Bubo*; Norberg, 1977), and cetaceans (e.g., *Monodon*, *Phocoena*; Ness, 1967; Yurick & Gaskin, 1988). If cranial asymmetries cannot be explained by injuries or disease states (see Howell, 1925), they are often proposed to offer a functional advantage (e.g., feeding efficiency; acoustic triangulation; Norberg, 1977; Benkman, 1996). In other studies, fluctuating asymmetry via intrinsic genetic factors has been identified in deep time (Goswami et al., 2015) as an explanation for developmental stability. This developmental integration, in concert with extrinsic environmental factors (Willmore et al., 2005), has also helped to explain some patterns of asymmetry observed in these groups.

To our knowledge, ours is the first study in which asymmetrical casque deviations have been classified among cassowaries. In
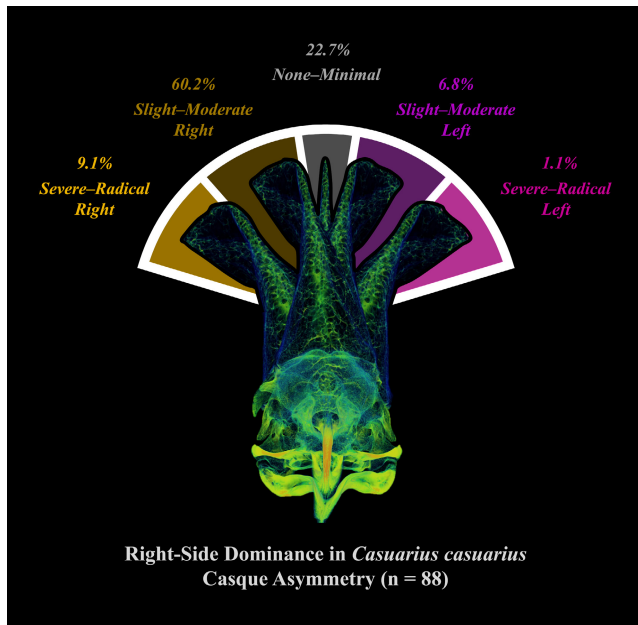
FIGURE 9 Figure summarizing the degree of deviation results (by percentage, rounded to the nearest tenth) for the *Casuarius casuarius* casque sample, which exhibited a right directional asymmetry. Micro-CT rendering of cassowary skull (green) pictured from rostral view, and various casque asymmetry positions superimposed. Deviation categories included: (1) none–minimal (0°–5° leftward/rightward; gray), (2) slight–moderate rightward (6°–30°; dark gold), (3) slight–moderate leftward (6°–30°; dark purple), (4) severe–radical rightward (31°–60°; light gold), and (5) severe–radical leftward (31°–60°; light purple).

cassowaries, asymmetric phenotypes occur as a combination of the casque's outer keratin sheath and the underlying bony core (Green & Gignac, 2021). Although casque asymmetry does not appear to develop systematically, as in the examples listed above, casque deviations provide important context about the potential variability of *C. casuarius* casque phenotypes. For example, PC1 in our rostral-shape analyses accounts for more than 50% of the variance in both sex-based (Figure 6) and geographic comparisons (Figure 8), indicating that asymmetry strongly influences the shape space that *C. casuarius* casques occupy.

Why most casques (98.2%) should become asymmetric in wild and captive *C. casuarius* is not immediately clear. It may be tempting to assume that directly vertical growth of the tall, narrow casques of *C. casuarius* either (1) is difficult to maintain against the force of gravity over time, (2) undergoes mechanical damage from walking through dense forests, or (3) heals asymmetrically due to fighting among conspecifics (agonistic behaviors such as charging, chasing, and kicking are common for cassowaries; Rothschild, 1900; Crome, 1976; Kofron, 1999). However, we do not interpret this to be this case. The exceptionally tall casques in our sample are non-deviated, indicating that the force of gravity over time is not necessarily a corollary of tallness. Additionally, we did not detect any pathologies of the keratinous sheathing or underlying bone that would indicate mechanical damage in deviated casques. Finally, the uneven (rightward biased)

directional asymmetry suggests a developmental bias, which could be due to nutritional availability, consistent environmental influences, genetic predisposition, functional advantage, or a combination of the four. For example, *C. casuarius* casques are thought to potentially function in thermoregulation (Eastick et al., 2019; Phillips & Sanborn, 1994), and casque deviations may play a role in optimizing the casque as a thermal window (depending on its positioning with the sun) that perhaps differs geographically or with altitude. On the other hand, proclivity for rightward asymmetry could reflect historic sampling biases for extravagant casques, unidentified factors from regional collection sites, or random chance in our specific sample. Asymmetries appear to be more common in later ontogeny; therefore, we recommend that a better understanding of how casques age in adults may help elucidate this issue.

4.4 | Support for social selection hypotheses

Ornamented, monomorphic species in which females and males appear comparable, as is the case for *C. casuarius*, are often considered to be under social selection (Schlupp, 2021), instead of the more narrowly defined sexual selection (West-Eberhard, 1983). Social selection is the phenomenon by which resource competition within populations leads to differential reproduction, regardless of the resource (West-Eberhard, 1983). When the resource is sex-specific, we describe this form of social selection as sexual selection (Schlupp, 2021; West-Eberhard, 1983). When sexual selection occurs by means of females and males both selecting mates, this is considered to be mutual sexual selection (see Hone et al., 2012; Huxley, 1914). The distinction between social selection and mutual sexual selection appears to pivot on whether or not females and males are making the same kind of choice (Schlupp, 2021). For example, actively selecting for tall casques versus actively selecting against short casques are different choices with different outcomes for, especially, individuals with middle-sized casques. In this hypothetical, social selection is the process by which female and male cassowaries select in the same way, whereas mutual sexual selection is the process by which females and males make sex-specific choices, even if the resulting patterns appear consistent. West-Eberhard (1983), who first investigated social selection as a mechanism for shaping unusual phenotypes, noted several common characteristics for species undergoing social selection. These include: (1) extreme physical traits that are (2) sexually monomorphic and (3) correlate to a species' social system. Cassowary casques fit this pattern well. They represent an extreme feature, and one that is dorsoventrally elongate in *C. casuarius*. Our data demonstrate that this exaggerated feature is sexually monomorphic with regard to shape. Additionally, these casques appear to hold utility for dominance signals that influence intraspecific competition (e.g., stretch display, see above). Finally, casque shapes vary between the three currently recognized cassowary species (Perron, 2016). This implies that the casque shape holds within-species significance and indicates that additional inter- and intraspecific comparisons may shed
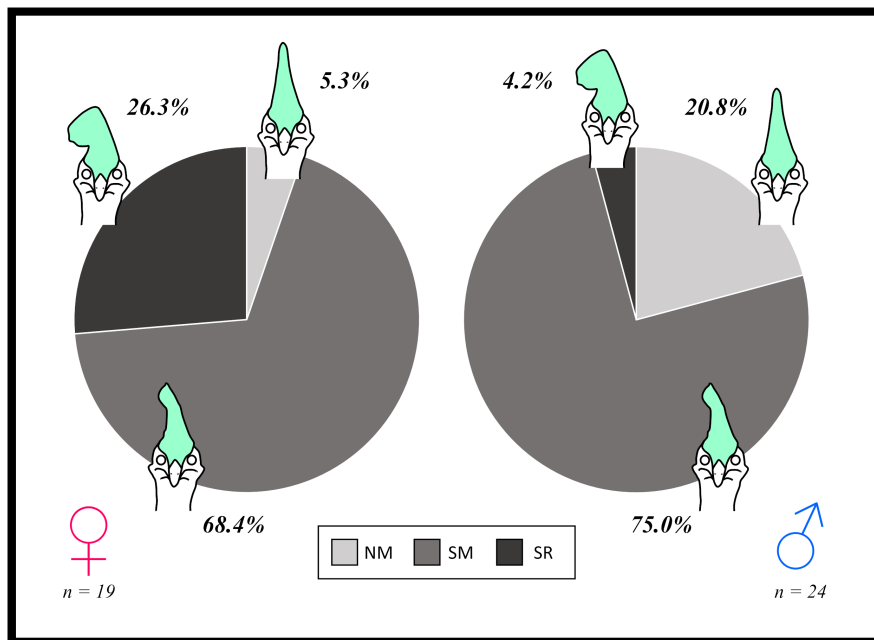
FIGURE 10 Pie charts summarizing degree of casque deviation results of known-sex *Casuarius casuarius* samples (left, female = pink symbol; right, male = blue symbol). Leftward and rightward deviation categories were combined into the following categories: (NM) none–minimal (0°–5° leftward/rightward; lightest gray), (SM) slight–moderate leftward/rightward (6°–30°; middle gray), (SR) severe– radical leftward/rightward (31°–60°; darkest gray). Superimposed cassowary icons (rostral views) represent degrees of casque asymmetry deviations (pastel green). Percentages are rounded to the nearest tenth and sample sizes are indicated (*n*) under each sex symbol.

further light on shape variation across *Casuarius*. Based on the findings herein, we recommend that social selection (Schlupp, 2021; West-Eberhard, 1983), generally, or mutual sexual selection (Hone et al., 2012; Huxley, 1914), more specifically, should be considered as viable hypotheses for shape variation in future studies tracing the development and evolutionary history of the casque (e.g., along with other hypotheses for visual-display functions, such as species recognition; West-Eberhard, 1983, 2005).

AUTHOR CONTRIBUTIONS
T. L. G. and P. M. G. conceived and designed the study, μCT scanned specimens, and wrote the manuscript. T. L. G., P. M. G., and D. I. K. provided analysis and interpretation of data, edited manuscript drafts, and devised figures. D. I. K. wrote and managed R code and constructed plots. T. L. G. collected photographic specimen data, managed specimen tables, and created figures for the manuscript.

DATA AVAILABILITY STATEMENT
Data available in article supplementary material

ORCID
Todd L. Green https://orcid.org/0000-0003-1407-6738
Paul M. Gignac https://orcid.org/0000-0001-9181-3258

REFERENCES

Andersson, M. (1994) *Sexual selection.* Princeton: Princeton University Press.

Angst, D., Barnoud, J., Cornette, R. & Chinsamy, A. (2020) Sex and ontogenetic variation in the crest of *Numida meleagris*: implications for crested vertebrates. *The Anatomical Record*, 303(4), 1018–1034.

Benkman, C.W. (1996) Are the ratios of bill crossing morphs in crossbills the result of frequency-dependent selection? *Evolutionary Ecology*, 10(1), 119–126.

Bentrupperbaumer, J. (1997) Reciprocal ecosystem impact and behavioural interactions between cassowaries, *Casuarius casuarius*, and humans, *Homo sapiens*: exploring the natural-human environment interface and its implications for endangered species recovery in North Queensland, Australia. PhD thesis, James Cook University.

BirdLife International and Handbook of the Birds of the World. (2019). Bird species distribution maps of the world. Version 2019.1. Available at: http://datazone.birdlife.org/species/requestdis.

Bitton, P.P. & Doucet, S.M. (2016) Sympatric black-headed and elegant trogons focus on different plumage characteristics for species recognition. *Animal Behaviour*, 116, 213–221.

Bolwig, N. (1973) Agonistic and sexual behavior of the African ostrich (*Struthio camelus*). *The Condor*, 75(1), 100–105.

Bonhomme, V., Picq, S., Gaucherel, C. & Claude, J. (2014) *Momocs*: outline analysis using R. *Journal of Statistical Software*, 56(13), 1–24.

Bubenik, G.A. & Bubenik, A.B. (1990) *Horns, pronghorns, and antlers: evolution, morphology, physiology, and social significance*. New York: Springer-Verlag.

Buchholz, R. (1991) Older males have bigger knobs: correlates of ornamentation in two species of curassow. *The Auk*, 108(1), 153–160.

Crome, F.H.J. (1976) Some observations on the biology of the cassowary in northern Queensland. *Emu*, 76(1), 8–14.

Crome, F.H.J. & Moore, L.A. (1988) The cassowary's casque. *Emu*, 88(2), 123–124.

Dakin, R. (2011) The crest of the peafowl: a sexually dimorphic plumage ornament signals condition in both males and females. *Journal of Avian Biology*, 42(5), 405–414.

Diamond, J. (1986) Biology of birds of paradise and bowerbirds. *Annual Review of Ecology and Systematics*, 17(1), 17–37.

Dodson, P. (1975) Taxonomic implications of relative growth in lambeosaurine hadrosaurs. *Systematic Biology*, 24(1), 37–54.

Darwin, C. (1871) *The descent of man, and selection in relation to sex*. London: John Murray.

Eastick, D.L., Tattersall, G.J., Watson, S.J., Lesku, J.A. & Robert, K.A. (2019) Cassowary casques act as thermal windows. *Scientific Reports*, 9(1), 1–7.

Felice, R.N. & O'Connor, P.M. (2014) Ecology and caudal skeletal morphology in birds: the convergent evolution of pygostyle shape in underwater foraging taxa. *PLoS One*, 9(2), e89737.

Flower, W.H. (1871) On the skeleton of the Australian cassowary (*Casuarius australis*). *Proceedings of the Zoological Society of London*, 3, 32–35.

Frith, C.B. (1978) The function of display and coloration in the sunbittern. *Avicultural Magazine*, 84(3), 150–157.

Gamble, K.C. (2007) Internal anatomy of the hornbill casque described by radiography, contrast radiography, and computed tomography. *Journal of Avian Medicine and Surgery*, 21(1), 38–49.

Gill, F.B. (2007) *Ornithology*, 3rd edition. New York: W. H. Freeman and Company.

Goswami, A., Binder, W.J., Meachen, J. & O'Keefe, F.R. (2015) The fossil record of phenotypic integration and modularity: a deep-time perspective on developmental and evolutionary dynamics. *Proceedings of the National Academy of Sciences*, 112(16), 4891–4896.

Grant, P.R. & Grant, B.R. (2009) The secondary contact phase of allopatric speciation in Darwin's finches. *Proceedings of the National Academy of Sciences*, 106(48), 20141–20148.

Green, T.L. & Gignac, P.M. (2021) Osteological description of casque ontogeny in the southern cassowary (*Casuarius casuarius*) using micro-CT imaging. *The Anatomical Record*, 304, 461–479.

Hagelin, J.C. (2002) The kinds of traits involved in male-male competition: a comparison of plumage, behavior, and body size in quail. *Behavioral Ecology*, 13(1), 32–41.

Hatch, J.J. (1985) Lateral asymmetry of the bill of *Loxops coccineus* (Drepanidinae). *The Condor*, 87(4), 546–547.

Hone, D.W., Naish, D. & Cuthill, I.C. (2012) Does mutual sexual selection explain the evolution of head crests in pterosaurs and dinosaurs? *Lethaia*, 45(2), 139–156.

Howell, A.B. (1925) Asymmetry in the skulls of mammals. *Proceedings of the United States National Museum*, 67(2599), 1–18.

Huxley, J.S. (1914) The courtship habits of the great crested grebe *Podiceps cristatus*; with an addition to the theory of sexual selection. *Proceedings of the Zoological Society of London*, 35, 491–562.

IUCN. (2020). The IUCN red list of threatened species. Version 2020-1. https://www.iucnredlist.org. Downloaded on 24 June 2020.

Jones, I.L. & Hunter, F.M. (1999) Experimental evidence for mutual inter- and intra-sexual selection favouring a crested auklet ornament. *Animal Behaviour*, 57(3), 521–528.

Kemp, A.C. (2001). Family Bucerotidae (hornbills). In: del Hoyo, J., Elliott, A., Sargatal J. (Eds.) *Handbook of the birds of the world*. Vol. 6. (Mousebirds to hornbills). Barcelona: Lynx Edicons, pp. 436–523.

Kinnaird, M.F., Hadiprakarsa, Y.Y. & Thiensongrusamee, P. (2003) Aerial jousting by helmeted hornbills *Rhinoplax vigil*: observations from Indonesia and Thailand. *Ibis*, 145(3), 506–508.

Kofron, C.P. (1999) Attacks to humans and domestic animals by the southern cassowary (*Casuarius casuarius johnsonii*) in Queensland, Australia. *Journal of Zoology*, 249(4), 375–381.

Lande, R. (1976) Natural selection and random genetic drift in phenotypic evolution. *Evolution*, 30, 314–334.

Lande, R. (1979) Quantitative genetic analysis of multivariate evolution, applied to brain: body size allometry. *Evolution*, 33, 402–416.

Marshall, W. (1872) Über die knöchernen Schädelhöcker der Vögel. *Niederländisches Archiv für Zoologie*, 1, 133–179.

Marugán-Lobón, J. & Buscalioni, Á.D. (2004) Geometric morphometrics in macroevolution: morphological diversity of the skull in modern avian forms in contrast to some theropod dinosaurs. In: *Morphometrics*. Berlin: Springer, pp. 157–173.

Mayr, G. (2018) A survey of casques, frontal humps, and other extravagant bony cranial protuberances in birds. *Zoomorphology*, 137(3), 457–472.

Naish, D. & Perron, R. (2016) Structure and function of the cassowary's casque and its implications for cassowary history, biology and evolution. *Historical Biology*, 28(4), 507–518.

Ness, A.R. (1967) A measure of asymmetry of the skulls of odontocete whales. *Journal of Zoology*, 153(2), 209–221.

Norberg, R.Å. (1977) Occurrence and independent evolution of bilateral ear asymmetry in owls and implications on owl taxonomy. *Philosophical transactions of the Royal Society of London B, Biological Sciences*, 280(973), 375–408.

Oksanen, J., Kindt, R., Legendre, P. and O'Hara, B. (2007). Vegan: community ecology package. R package version 1.8-5. Available at: http://cran.r-project.org/.

Olson, V.A. & Turvey, S.T. (2013) The evolution of sexual dimorphism in New Zealand giant moa (*Dinornis*) and other ratites. *Proceedings of the Royal Society B: Biological Sciences*, 280(1760), 20130401.

Parker, W.K. (1866) VIII. On the structure and development of the skull of the ostrich tribe. *Proceedings of the Zoological Society of London*, 14, 112–114.

Perron, R.M. (2016) *Taxonomy of the genus Casuarius: the defined and known living cassowary species and subspecies.* United Kingdom: Quantum Conservation.

Phillips, P.K. & Sanborn, A.F. (1994) An infrared, thermographic study of surface temperature in three ratites: ostrich, emu and double-wattled cassowary. *Journal of Thermal Biology*, 19(6), 423–430.

Pycraft, W.P. (1900) On the morphology and phylogeny of the palæognathæ (ratitæ and crypturi) and neognathæ (carinatæ). *The Transactions of the Zoological Society of London*, 15(5), 149–290.

R Core Team. (2020) *R: a language and environment for statistical computing.* Vienna: R Foundation for Statistical Computing.

Raikow, R.J. (1969) Sexual and agonistic behavior of the common Rhea. *The Wilson Bulletin*, 81(2), 196–206.

Ripley, B. (2013): R package MASS. http://www.cran.r-project.org/package=MASS

Rothschild, W. (1900) A monograph of the genus *Casuarius*. *The Transactions of the Zoological Society of London*, 15(5), 109–148.

Schlupp, I. (2021) *Male choice, female competition, and female ornaments in sexual selection.* Oxford: Oxford University Press.

West-Eberhard, M.J. (1983) Sexual selection, social competition, and speciation. *The Quarterly Review of Biology*, 58(2), 155–183.

West-Eberhard, M.J. (2005) Developmental plasticity and the origin of species differences. *Proceedings of the National Academy of Sciences*, 102(suppl. 1), 6543–6549.

Willmore, K.E., Klingenberg, C.P. & Hallgrímsson, B. (2005) The relationship between fluctuating asymmetry and environmental variance in rhesus macaque skulls. *Evolution*, 59(4), 898–909.

Wright, S. (1945) Tempo and mode in evolution: a critical review. *Ecology*, 26, 415–419.

Yurick, D.B. & Gaskin, D.E. (1988) Asymmetry in the skull of the harbour porpoise *Phocoena phocoena* (L.) and its relationship to sound production and echolocation. *Canadian Journal of Zoology*, 66(2), 399–402.

SUPPORTING INFORMATION

Additional supporting information can be found online in the Supporting Information section at the end of this article.